*Geomechanics and Engineering, Vol. 2, No. 3 (2010) 161-176*
DOI: http://dx.doi.org/10.12989/gae.2010.2.3.161 

# The effectiveness of geosynthetic reinforcement, tamping, and stoneblowing of railtrack ballast beds under dynamic loading: DEM analysis

Sebastian Lobo-Guerrero[1] and Luis E. Vallejo*[2]

[1]*American Geotechnical & Environmental Services, Inc., Canonsburg, PA, U.S.A.*
[2]*Department of Civil and Environmental Engineering, University of Pittsburgh, 949 Benedum Hall, Pittsburgh, PA 15261, U.S.A.*

*(Received March 16, 2010, Accepted August 11, 2010)*

**Abstract.** Discrete Element Method (DEM) simulations were developed to investigate the effectiveness of geosynthetic reinforcement and the effectiveness of maintenance techniques performed on a simulated ballast bed subjected to dynamic loading. The results from four samples subjected each one to a total of 425 load cycles are presented: one unreinforced and unmaintained sample, one unmaintained but reinforced sample, one unreinforced sample subjected to maintenance in the form of stoneblowing after 200 load cycles, and one unreinforced sample subjected to maintenance in the form of tamping after 200 load cycles. The obtained values of permanent deformation as a function of the applied number of load cycles for the four cases are presented together allowing a comparison of the effectiveness of each technique. Moreover, snapshots of the simulated track sections are presented at different moments of the simulations. The simulations indicated that the geosynthetic reinforcement may not be beneficial for the analyzed case while stoneblowing was the most effective maintenance technique.

**Keywords:** railtracks; ballast; particle crushing; tamping; stoneblowing; geosynthetics; discrete element method; numerical analysis.

## 1. Introduction

A rail track ballast bed is made of crushed rock, nickel slag or crushed gravel. It is composed by strong and durable particles having sizes typically between 0.25in (6.4 mm) and 2.5in (64 mm). During its serviceable life, the ballast bed is subjected to cyclic loads. As a result of this, ballast densification, aggregate degradation, and lateral spread of the ballast material underneath the ties takes place inducing permanent deformations on the railway (Raymond and Bathurst 1987). As reported by Indraratna *et al.* (1998), maintenance and rehabilitation costs of railtracks due to problems related with ballast performance are substantial, and millions of dollars are annually spent around the world in these activities. Understanding the degradation process of the ballast bed and the effectiveness of the used maintenance techniques could lead to the design of better railways reducing these costs.

*Corresponding author, Professor, E-mail: vallejo@pitt.edu

Discrete Element Method (DEM) simulations were developed to study the effectiveness of reinforcing an original undamaged ballast bead with a geosynthetic fabric. Also, the effectiveness of performing different maintenance techniques to an unreinforced ballast bed that has deteriorated as a result of dynamic loading is evaluated. This study is a continuation of a previous work reported by the authors (Lobo-Guerrero and Vallejo 2006a) where an initial ballast bed forming part of a simulated track section was subjected to 200 load cycles. This new work starts from here applying 225 more load cycles to the simulated ballast bead (a cumulative of 425 load cycles). Moreover, a copy of the original ballast bed in its initial state was reinforced using a geosynthetic fabric and it was subjected to 425 load cycles. A comparison between the response of the reinforced and the unreinforced ballast beds is presented in terms of the induced permanent deformations after dynamic loading. In order to study the effectiveness of different maintenance techniques, stoneblowing and tamping were separately performed to two copies of the unreinforced ballast bed after the initial 200 load cycles. These two samples were subjected again to 225 load cycles after maintenance (cumulative of 425 load cycles). The effectiveness of each technique was measured in terms of permanent deformation as a function of the applied number of cycles.

## 2. Railtrack ballast, geosynthetic reinforcment, and maintenance techniques

Economic factors such as production, transportation, placement, and maintenance costs need to be considered when selecting a specific track ballast (Klassen *et al.* 1987). Moreover, the material properties need to be evaluated and compared with standards. Typical specifications for track ballast include ranges of acceptable values of bulk specific gravity, gradation, percentage of fractured particles, resistance to weathering (Magnesium soundness, absorption), and resistance to degradation (Los Angeles abrasion, mill abrasion) (CP Rail Specification for Ballast 1987).

Maintenance of the ballast bed is usually performed after significant permanent deformations have been reached on the rail track. The purpose of maintenance is to reset the level and/or alignment of the track. Tamping is a common maintenance operation consisting on lifting the sleepers to the correct level and vibrating the material underneath with metal spikes. The induced vibrations produce movement of the ballast particles and dilation of the material. After the railtrack is in service again and is dynamically loaded, the ballast contracts and a deformation pattern similar to the one obtained before maintenance develops with time. This is known as "ballast memory" (Anderson and Key 2000, McMichael and McNaughton 2003). Stoneblowing is another maintenance technique. It starts with the lifting of the sleepers to correct level and alignment. After this, small gravel particles are blown with compressed air into the gap formed between the sleeper and the ballast bed. Previous experience has shown that 14-20 mm gravel particles are the preferred small stone used for stoneblowing (Anderson and Key 2000, McMichael and McNaughton 2003).

The use of geosynthetics to reinforce the structure of ballast beds is another option that has been recently explored. For example, McDowell and Stickley (2006) showed that the inclusion of a geogrid (at one third of the bed thickness measured from the base) could significantly reduce the permanent deformation induced on an experimentally simulated ballast bed (box test) loaded under dynamic conditions. They found that the produced improvement was more significant on good quality ballast than in much more crushable ballast. The use of the geogrid did not prevent particle breakage, which was a very important cause of permanent deformation for the crushable ballast. They also found that the use of the geogrid could help to reduce the number of maintenance events.

Thus, the use of geosynthetic reinforcement can help to prevent significant permanent deformations if performed under certain circumstances.

## 3. Studing the behavior of ballast under track conditions using DEM

Previous research has shown that DEM can be satisfactorily used to study the behavior of ballast under track conditions (Lim and McDowell 2005, Lobo-Guerrero and Vallejo 2006a). The PFC$^{2D}$ program which is based on DEM was used in this study. In this program particles are idealized as discs that interact with each other at their contacts. This interaction is mainly governed by two models: the stiffness model and the slip model (ITASCA 2002). Since the original DEM developed by Cundall and Strack (1979) considers unbreakable particles, a particle breakage model has been developed and implemented by the authors to allow particle breakage. The details and background of the adopted model have been presented in previous articles (Lobo-Guerrero and Vallejo 2005a, 2005b, 2005c, 2005d, 2006a, 2006b). Only the main assumptions of the model are summarized:

- Only particles with a coordination number equal to or smaller than 3 are able to be broken.
- For those particles having a coordination number smaller than or equal to 3, the loading configuration such as the one presented in Fig. 1(a) is assumed to be equivalent to a Brazilian test, as shown in Fig. 1(b). The induced tensile stress, $\sigma_t$, can be obtained with the expression presented on Fig. 1(b), where $P_1$ is the value of the highest contact force acting on the particle, $L$ is the thickness of the disk (unit thickness for the simulated case), and $D$ is the diameter of the disk.
- The tensile strength of a particle having a radius of 1 mm is predefined as $\sigma_{max1mm}=3\times10^6$ Pa, and is assumed that the tensile strength of a particle with a radius $r$, $\sigma_{max}(r)$, is related to $\sigma_{max1mm}$ according to $\sigma_{max}(r)=\sigma_{max1mm}[r]^{-1}$ (where $r$ is expressed in mm/mm since it needs to be normalized by the reference value of 1 mm).
- Every particle with a coordination number smaller than or equal to 3 is allowed to break if $\sigma_t > \sigma_{max}(r)$.

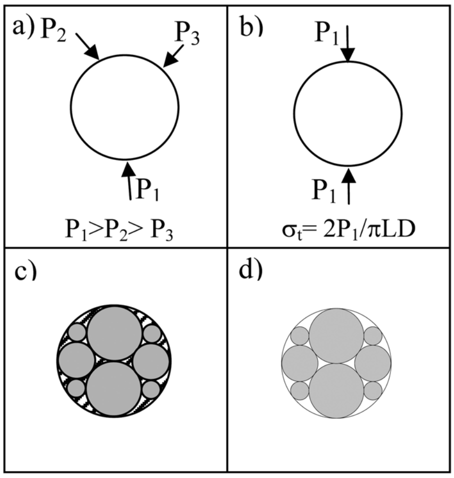


Fig. 1 Idealization of the induced tensile stress and the produced fragments after failure

When a particle fulfills the failure criterion, it breaks into 8 fragments having 3 different sizes as shown on Fig. 1(c), and many fines represented by the dashed area in the figure. As experimentally observed by McDowell *et al.* (2004), fine particles produced due to ballast breakage migrate through the pore spaces between the surrounding particles and move to the bottom of the ballast bed. Thus, for the sake of computer efficiency this material is not considered in the model. Only 8 fragments are considered to replace the broken particle as illustrated on Fig. 1(d).

This particle breakage model has been implemented to PFC$^{2D}$ (using the FISH language) by Lobo-Guerrero and Vallejo, and it has been used to analyze the evolution of crushing in granular materials subjected to different conditions of stress and strain such as direct shear tests, ring shear tests, isotropic and deviatoric stress paths in biaxial tests, and penetration tests. The implemented function automatically checks for particles fulfilling the failure criterion. If a particle is fulfilling the failure criterion, information such as position and radius are stored, and the particle is deleted. After this, the subroutine automatically generates the fragments based on the stored information and the simulation continues. The properties of the new fragments are similar to those from the breaking particle. The subroutine does not restrict smaller particles from continuing to break. Thus, different generations of crushing coexist inside the simulated granular material.

## 4. Configuration of the simulated material and initial loading: previous work

A simulated box container having a width of 2.1 m, and a height of 0.6 m was created. The coefficients of normal and shear stiffness of the walls forming this box were set to $1\times10^9$ N/m, and their friction coefficients were set to 0.7. After this, particles with a radius of 2 cm were randomly generated inside the box with the constraint of no overlaps between them. The density of these particles was set to 2500 kg/m$^3$, and their coefficients of normal and shear stiffness were set to $1\times10^8$ N/m. Their friction coefficient was also set to 0.7. These particles were allowed to settle under a gravity field (9.8 m/s$^2$). After this, compaction was induced by vertically moving the upper horizontal wall. This compaction continued until the maximum contact force in the material was approaching the value required to produce particle breakage. After this, the upper horizontal wall was moved upwards unloading the sample. This wall was deleted when it separated from the upper part of the simulated ballast material.

The simulated 3 sleepers had a width of 30 cm, a height of 15 cm, and a length of 1 m. Fig. 2 shows the geometry of the simulated rail track section. The separation between the sleepers was equal to 30 cm. Also, the distance between the external sleepers and the vertical boundaries of the container was equal to 30 cm. The sleepers were placed over a 45 cm ballast bed. They were artificially embedded inside the ballast by deleting some particles. The final sample was composed by 639 ballast particles. The friction coefficient and the coefficients of normal and shear stiffness of the sleepers were equal to those used for the walls forming the box container. The 3 sleepers were idealized as only one body since they were not allowed to have differential settlements between each other. The rail and connections to the sleepers shown on Fig. 2 were added to the figure after the simulations, they are shown only to help the reader to understand the configuration of the track section. The "invisible" real rigid connection between the three sleepers was programmed in the numerical model. The seating of the sleepers was carried out by vertically moving them until the maximum contact force developed in the ballast was half the value required to produce particle breakage. After this, the sleepers were unloaded and the reference point for measuring permanent

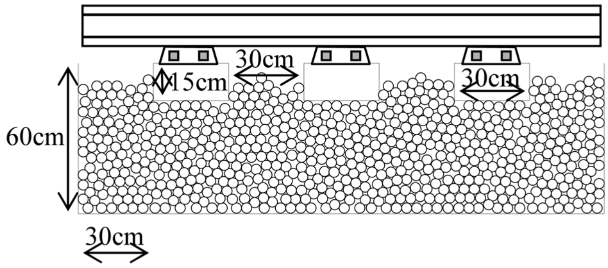


Fig. 2 Geometry of the simulated track section

deformation was fixed.

A FISH function was programmed by the authors in order to induce the cyclic loading. The programmed servo-mechanism vertically moved the 3 sleepers at a velocity equal to $5\times10^{-7}$ m/step until the total applied force was equal to 62 kN, then, the 3 sleepers were unloaded at the same velocity until no load was applied to them. This cyclic loading and unloading continued until the first 200 cycles were completed. More details about the generation of the sample, the compaction process, the seating of the sleepers, and the loading mechanism can be found in Lobo-Guerrero and Vallejo (2006a).

The permanent deformation at the end of the 200 cycles was equal to 5.12 cm. This non-recoverable deformation was the result of particle rearrangement and particle crushing. Particle crushing was observed underneath the sleepers. However, no more than a third generation of crushing was found inside the sample. The generation of crushing represents the number of breakage events that a particle has experienced. Thus, the fragments produced as a result of crushing of the original particles are called first generation of crushing, the fragments coming from these fragments are referred as a second generation of crushing, and so on. The first snap shot of Fig. 3 shows the sample at the end of the initial 200 load cycles.

## 5. Unreinforced and reinforced samples

### 5.1 Unreinforced ballast bed

A copy of the sample after the initial 200 load cycles was subjected to 225 more cycles. This "control section" shows the effect of the total 425 uninterrupted load cycles on the unreinforced ballast bed. Fig. 3 shows snapshots of the simulated railtrack section at different moments of the simulation (this sample was referred as the no maintenance case to avoid confusion with the other simulations). Particle crushing continued to occur during the extra 225 load cycles, concentrating underneath the ties. However, no more than a third generation of crushing was found inside the sample. Szymoniak (1986) and Pitner *et al.* (1987) report that the production of fines in samples of basalt subjected to 100,000 cycles of loading takes place at the beginning of the test (about 500 cycles), with very little degradation occurring as the number of cycles increases. The percentage by weight of fines after the 100,000 load cycles was only 0.9% of the original weight of the samples. Most of the fines were produced at the beginning of the cyclic loading. For this reason, in this study the number of load cycles was chosen as 425.

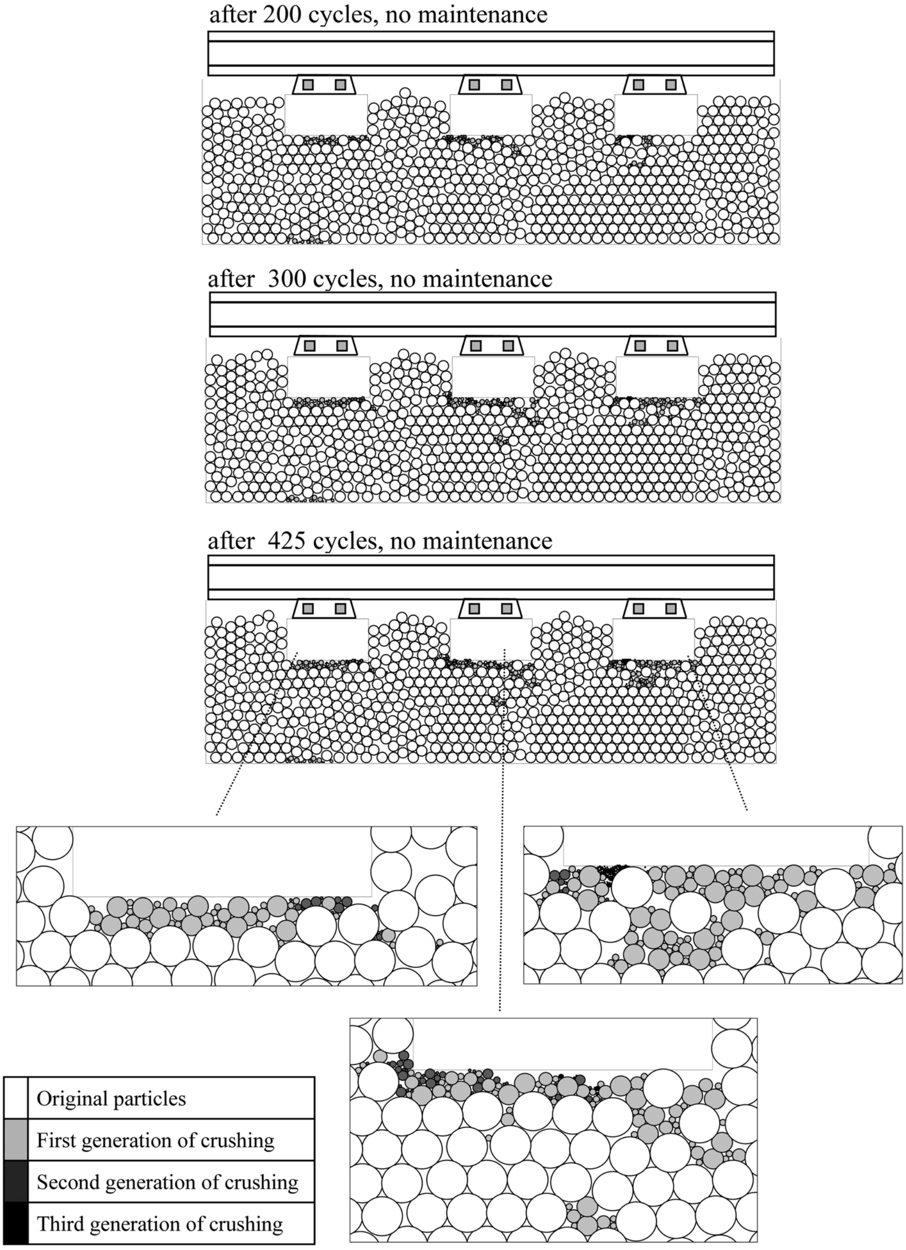


Fig. 3 Control section: no maintenance

The obtained values of permanent deformation as a function of the total applied number of cycles are shown in Fig. 4 as the "no maintenance case". This figure also shows the values obtained for the reinforced sample and the samples subjected to maintenance in the form of stoneblowing and tamping as discussed later on the next sections. Fig. 4 shows that the rate of increment on permanent deformation considerably reduced as the applied number of cycles increased. After around 300 cycles, the sample tended to stabilized and it reached a permanent deformation equal to

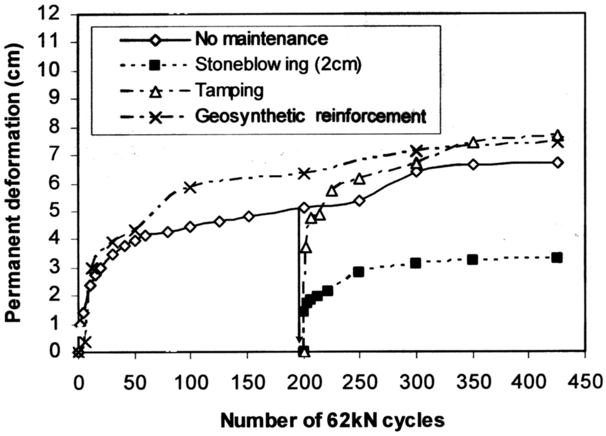


Fig. 4 Permanent deformation vs. applied number of load cycles: summary of the research program

6.72 cm after 425 cycles. The following sections present a comparison with the results obtained when some alterations such as the inclusion of a geosynthetic reinforcement or track maintenance were considered.

### *5.2 Reinforced ballast bed*

A copy of the initial sample after compaction and seating of the sleepers was modified to include the geosynthetic reinforcement. A FISH subroutine was developed by the authors in order to elevate the upper ballast particles and the sleepers, generating a gap at one third of the bed thickness (15 cm). McDowell and Stickley (2006) showed that placing the reinforcement at this height produced the best results when conducting experimental box tests on geogrid reinforced samples. Another FISH subroutine developed by the authors was used to generate the geosynthetic. This process is shown on Fig. 5(a) and Fig. 5(b). The geosynthetic was composed by two rows of bonded particles with a diameter of 2 mm. A total of 2099 particles formed the geosynthetic. The density, coefficients of normal and shear stiffness, and friction coefficient of these particles were similar to those used for the ballast particles. These particles were bonded together, allowing bending of the geosynthetic but not breakage due to tensile or shear forces. The particles forming the geosynthetic were also not allowed to crush. Previous research has shown that it is possible to successfully simulate the behavior of gesoynthetic materials using DEM such as geosynthetic anchorages (Villard and Chareyre 2004, Chareyre and Villard 2005), thin tunnel liners (Tannant and Wang 2004), and geo-composite cells (Bertrand *et al*. 2005).

After the geosynthetic was in place, the elevated particles were allowed to fall on top of it. Also, the sleepers were moved down. A second seating of the sleepers was done using the same procedure outlined before. Since the geosynthetic had no resistance to bending, it deformed following the profile of the particles as shown on Fig. 5(c). Thus, the disturbance of the initial ballast bed was minimized, and the sample obtained at the end of the process had a similar fabric to the original unreinforced sample. The reinforced sample was then subjected to 425 uninterrupted load cycles.

Fig. 6 shows snapshots of the reinforced sample after different number of applied load cycles.

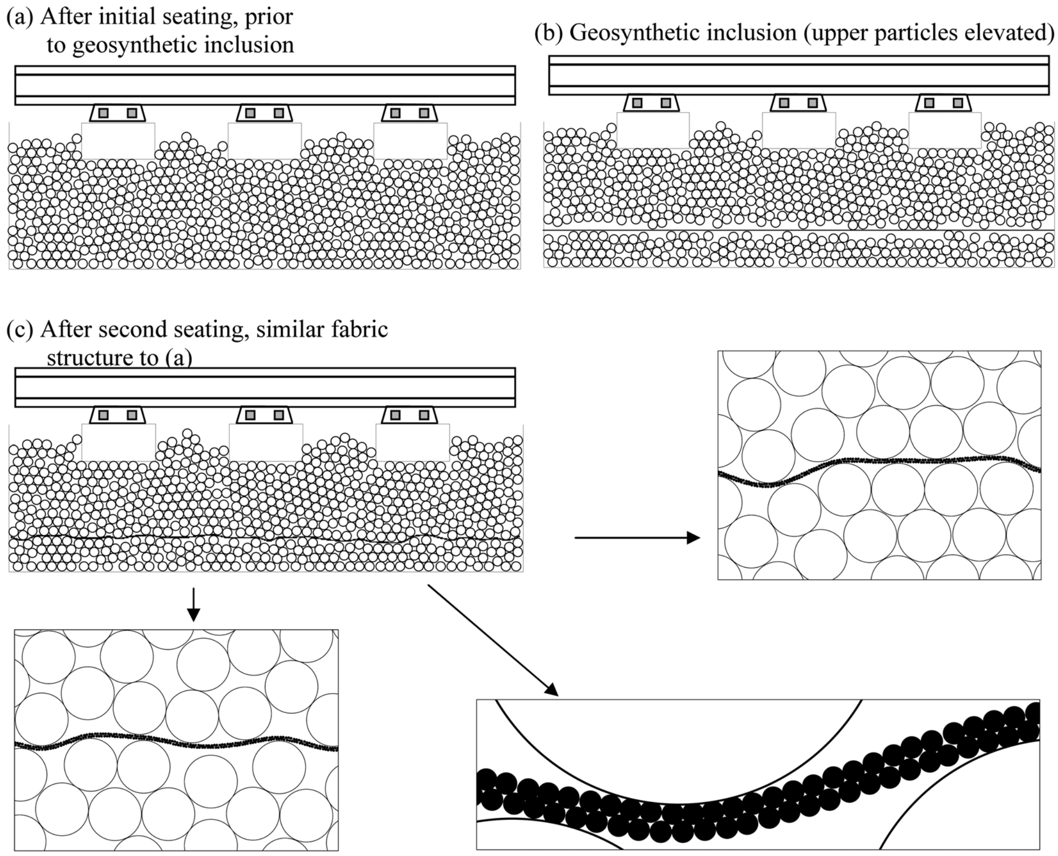


Fig. 5 Inclusion of the geosynthetic

Particle breakage concentrated underneath the sleepers, generating up to a third generation of crushing similarly to the unreinforced case. Fig. 7 shows an example of the force chains that developed inside the simulated material as a result of the applied load. This figure shows a pattern very similar to the one observed for the unreinforced case as reported by the authors in previous works (Lobo-Guerrero and Vallejo 2006a, Vallejo and Chik 2009). Vertical force chains transmitted most of the applied load from the sleepers to the bottom of the ballast bed. Crushing concentrated underneath the sleepers since the particles located in these regions had to bear large contact forces and had low values of coordination number due to geometrical constraint of being in contact with a flat surface. The presence of the geosynthetic did not alter the expected pattern since the vertical force chains passed through it.

Amplified details on Fig. 7 show typical examples of the forces that developed inside the geosynthetic. As expected some parts of the geosynthetic were subjected to tensile forces. The fact that the geosynthetic takes tensile forces could help to reduce the obtained values of permanent deformation since it could avoid further particle rearrangement. However, this was not the case for the analyzed sample. As shown on Fig. 4, the permanent deformation at the end of the 425 cycles was equal to 7.45 cm, a value that is slightly higher than the one obtained for the unreinforced case. In fact Fig. 4 shows that after 300 load cycles the two curves were very similar, tending to stabilize

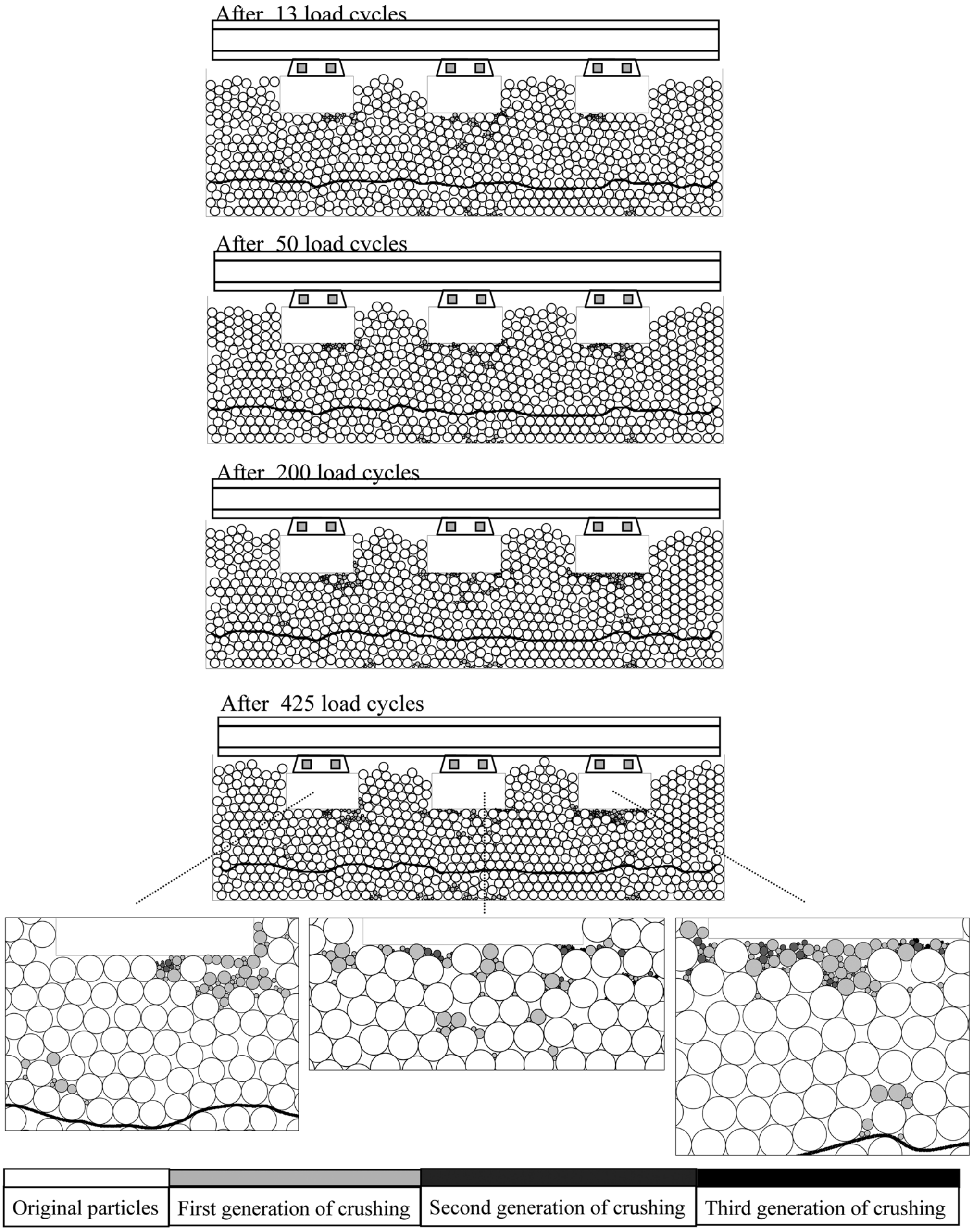


Fig. 6 Snap shots of the reinforced sample

around a permanent deformation of 7 cm. The two curves were also very similar during the first 50 load cycles, showing that the samples had a comparable initial fabric. A difference on the two curves appeared between 50 and 300 cycles, showing that crushing evolved slightly different in time inside the simulated samples. Nevertheless, both samples reached an almost steady state between 300 and 425 cycles, showing that the geosynthetic did not contribute to the stability of the sample

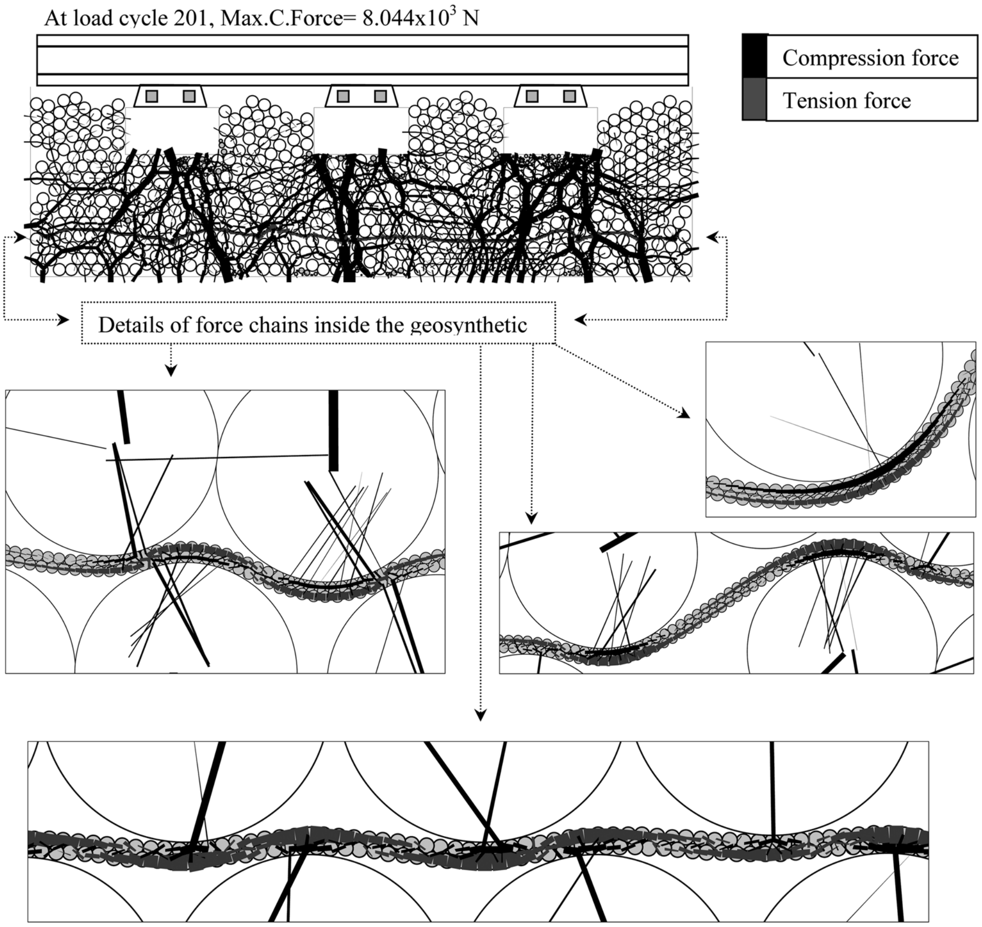


Fig. 7 Generated force chains: reinforced sample

and its associated permanent deformation. This can be explained since particle crushing, and the associated particle rearrangement between the unbroken particles and the generated fragments, were the principal mechanisms that contribute to the accumulation of permanent deformation. Thus, the inclusion of the geosynthetic did not effectively attack the cause of the problem. The following section explores the possibility of improving the performance of the simulated ballast bed using maintenance techniques. Only the unreinforced case is considered.

## 6. Maintenance of the unreinforced ballast bed after initial loading

### *6.1 Stoneblowing*

A copy of the unreinforced sample that experienced the initial 200 load cycles was subjected to stoneblowing. In order to correct the produced permanent deformation, the sleepers were lifted up to their initial position (no permanent deformation position). Then, small particles with a diameter of 2

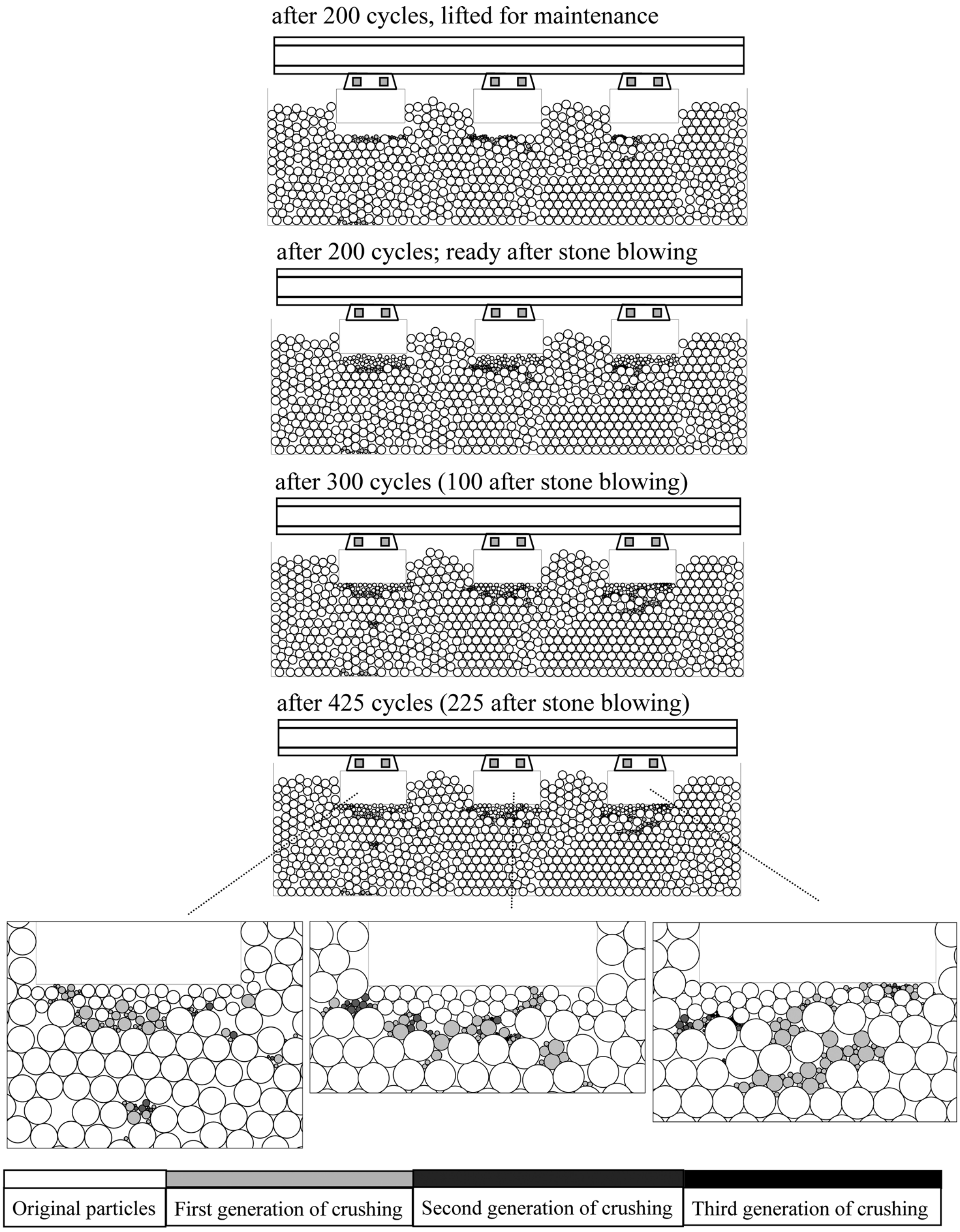


Fig. 8 Sample subjected to stoneblowing

cm were inserted into the gap between the bottom of the sleepers and the top of the deformed ballast bed. This process is shown on the first two snapshots of Fig. 8. Particles were randomly generated in the mentioned region with the constraint of no overlaps between them or with the old particles. The properties of the new small particles were equal to the properties of the old ballast.

After stoneblowing was performed to the sample, it was subjected to 225 more cycles. The loading mechanism was the same one used before. Thus, at the end of the simulation the sample had experienced a total of 425 load cycles. Fig. 8 shows some snap shots after different number of load cycles. The introduced small particles rearranged with each other and the old particles providing good support for the sleepers. As shown on this figure, some permanent deformation was induced as a result of the initial rearrangement of the introduced material (compaction). Fig. 8 shows that some crushing occurred underneath the sleepers but it was not a dominant factor during the simulation as opposed to the previous cases. The particles introduced during the stoneblowing were initially colored white since they had not experienced crushing at the track. Only a few of these particles experienced crushing during the simulation. The produced fragments were colored according to the generation that they represented. No more than a third generation of crushing for the whole sample was found. The introduced particles with the stoneblowing did not percolate through the voids between the surrounding particles, validating the size selection for the stoneblowing material.

As shown in Fig. 4, the unreinforced sample subjected to stoneblowing had the smallest value of permanent deformation at the end of the 425 load cycles (225 after stoneblowing). This permanent deformation was equal to 3.28 cm. A smaller settlement was produced during the last 225 load cycles compared to the initial 200 load cycles. After stoneblowing, the material deformed during approximately 50 cycles, but it quickly stabilized with almost no deformation during the following cycles.

### 6.2 Tamping

Another copy of the unreinforced sample that experienced the initial 200 load cycles was subjected to tamping. Similarly to the stoneblowing case, the sleepers were lifted up to the position of no permanent deformation. Tamping of the material directly underneath the sleepers was artificially simulated by moving selected particles and allowing them to settle and reorganize. Thus, the material dilated and made contact with the lifted sleepers. After this, the sample was subjected to 225 load cycles (reaching a total of 425 load cycles). The loading mechanism was the same one used during the previous 200 load cycles.

Fig. 9 shows snapshots at different moments of the simulation and amplified details of the sample at the end of the test. This figure shows that the material that was rearranged during tamping, rapidly contracted, producing permanent deformation underneath the sleepers. Moreover, significant particle crushing occurred, producing considerable permanent deformation. This was somehow expected since tamping produced a loose structure of the disturbed ballast material underneath the ties. Particles in these regions were very prone to break since they were subjected to large tensile stresses as a result of the lack of confinement. These tensile stresses would not develop in particles surrounded by more neighbors (dense structure). Fig. 9 shows that up to a fourth generation of crushing developed inside the sample, being the maximum generation of crushing found in this study.

Fig. 4 shows that tamping was not as effective as stoneblowing. The sample subjected to tamping had a deformation of 7.65 cm at the end of the total 425 load cycles. This permanent deformation was considerably higher than the one obtained on the sample subjected to stoneblowing. Also, more permanent deformation occurred during the 225 load cycles after tamping than during the initial 200 cycles as opposed to the stoneblowing case. A comparison with the results from the unreinforced

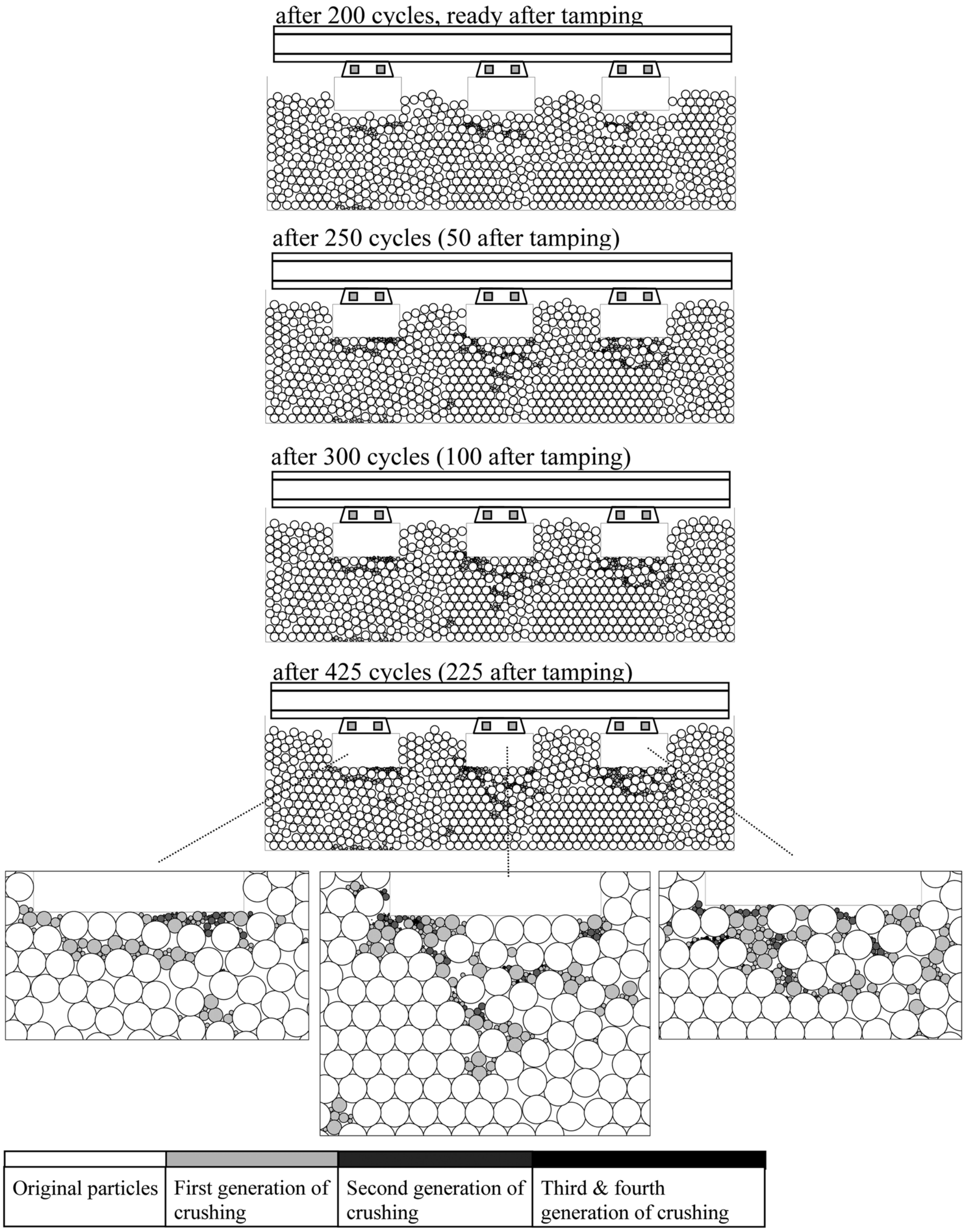


Fig. 9 Sample subjected to tamping

and unmaintained sample and the results from reinforced sample shows ballast memory. The disturbed and dilated ballast material after tamping quickly contracted and followed almost the same curves of the undisturbed sample and the reinforced sample. However, the curve showing the results from the sample subjected to tamping is slightly up than the other two. This is due to the permanent deformation generated by crushing during the first cycles after tamping. It is a consequence of disturbing an already compacted and consolidated material.

## 7. Limitations of the simulations

There is always a compromise between reality and the feasibility of the modeling approach. For this study many assumptions were taken since they were the only possible alternatives. It is important to understand the limitations that these assumptions may represent. The most important limitation corresponds with the constraint that only circular disks were considered. It is well known that rounded particles are not the best ballast, and should be avoided when possible (Raymond 2000). Circular disks do not represent the angularity of ballast particles which has been found to be the key component controlling friction and interlock within a given gradation (Indraratna *et al.* 2006). Also, during ballast loading, the sharp corners of the particles break, which in turn affect the permanent deformation of the ballast (Mittal *et al.* 2009). The breakage of the corner of the particles is not simulated by the simulation that uses circular disks. Thus, the obtained values of permanent deformation in the simulations does not take into consideration the angularity, interlocking, and corner breaking that takes place in real ballast.

Another finding of the simulations presented in this study indicated that the geosynthetic reinforcement may not be beneficial to decrease permanent deformations in ballast subjected to cyclic loads. This finding was arrived at after comparing permanent deformations experienced by unreinforced and reinforced ballast samples. Both samples recorded similar deformations. The permanent deformations were the result of particle crushing underneath the ties, and the associated particle rearrangement between the unbroken particles and the generated fragments. Thus, the inclusion of the geosynthetic reinforcement may not effectively attack the cause of the problem. This result is in agreement with the experimental findings reported in the literature (McDowell and Stickley 2006). However, results obtained by Indraratna *et al.* (2006) and Mittal *et al.* (2009) seem to contradict the result of the simulations. Thus, there is no general agreement about the influence of geosynthetics in preventing permanent deformations in ballast. More research is needed to clarify this issue.

The numerical values obtained during the simulations should be treated with caution. Since the simulations were developed more for comparative purposes this may not be a critical factor.

## 8. Conclusions

The simulations presented in this study indicated that the use of the geosynthetic reinforcement may not be beneficial to decrease permanent deformations in ballast subjected to cyclic loads. This finding was arrived at after comparing permanent deformations experienced by unreinforced and reinforced ballast samples. Both samples recorded similar deformations. The permanent deformations were the result of particle crushing underneath the ties, and the associated particle rearrangement between the unbroken particles and the generated fragments. Thus, the inclusion of the geosynthetic may not effectively attack the cause of the problem. This is in agreement with the experimental findings reported in the literature (McDowell and Stickley 2006). However, results obtained by Indraratna *et al.* (2006) and Mittal *et al.* (2009) seem to contradict the result of the simulations. On the other hand, the results obtained for the sample subjected to maintenance in the form of stoneblowing showed that this technique was very effective. By introducing smaller particles to the ballast bed without disturbance, stoneblowing provides a very good support for the sleepers, resulting on lower values of permanent deformation and extended periods of serviceable life. The same could not be said for the sample subjected to maintenance in the form of tamping since problems related with ballast memory were observed. After some cycles, the sample reached similar values to those exhibited by the undisturbed and the reinforced samples. The above findings should be used with caution since the circular disks used in the simulations does not simulate completely the shape of the particles that form a real ballast.

## Acknowledgements

This work was supported by Grant No.CMS-0301815 to the University of Pittsburgh from the National Science Foundation, Washington, D.C. This support is gratefully acknowledged.

## References

Anderson, W.F. and Key, A.J. (2000), "Model testing of two-layer railway track ballast", *J. Geotech. Geoenviron. Eng. - ASCE*, **126**(4), 317-323.

Bertrand, D., Nicot, F., Gotteland, P. and Lambert, S. (2005), "Modelling a geo-composite cell using discrete analysis", *Comput. Geotech.*, **32**, 564-577.

Chareyre, B. and Villard, P. (2005), "Dynamic spar elements and discrete element methods in two dimensions for the modeling of soil-inclusion problems", *J. Eng. Mech. - ASCE*, **31**(7), 689-698.

CP Rail Specification for Ballast (1987), *Appendix of the transportation research record*, **1131**, 59-63.

Cundall, P.A. and Strack, O.D.L. (1979), "A discrete numerical model for granular assemblies", *Geotechnique*, **29**(1), 47-65.

Indraratna, B., Ionescu, D. and Christie, H.D. (1998), "Shear behavior of railway ballast based on large-scale triaxial tests", *J. Geotech. Geoenviron. Eng. - ASCE*, **124**(5), 439-449.

Indraratna, B., Khabbaz, H., Salim, W. and Christie, D. (2006), "Geotechnical properties of ballast and the role of geosynthetics in rail track stabilization", *Ground Improvement*, **10**(3), 91-101.

Itasca Consulting Group, Inc. (2002), *PFC$^{2D}$ (Particle Flow Code in Two Dimensions) version 3.0; sections: Theory and Background*; *FISH in PFC*.

Klassen, M.J., Clifton, A.W. and Watters, B.R. (1987), "Track evaluation and ballast performance specifications", *Transport. Res. Record*, **1131**, 35-44.

Lim, W.L. and McDowell, G.R. (2005), "Discrete element modelling of railway ballast", *Granular Matter*, **7**, 19-29.

Lobo-Guerrero, S. and Vallejo, L.E. (2005a), "Crushing a weak granular material: experimental numerical analyses", *Geotechnique*, **55**(3), 245-249.

Lobo-Guerrero, S. and Vallejo, L.E. (2005b), "Analysis of crushing of granular material under isotropic and biaxial stress conditions", *Soils Found.*, **45**(4), 79-87.

Lobo-Guerrero, S. and Vallejo, L.E. (2005c), "Discrete element method evaluation of granular crushing under direct shear test conditions", *J. Geotech. Geoenviron. Eng. - ASCE*, **131**(10), 1295-1300.

Lobo-Guerrero, S. and Vallejo, L.E. (2005d), "DEM analysis of crushing around driven piles in granular materials", *Geotechnique*, **55**(8), 617-623.

Lobo-Guerrero, S. and Vallejo, L.E. (2006a), "Discrete element method analysis of railtrack ballast degradation during cyclic loading", *Granular Matter*, **8**(3-4), 195-204.

Lobo-Guerrero, S. and Vallejo, L.E. (2006b), "Modeling granular crushing in ring shear tests: experimental and

numerical analyses", *Soils Found.*, **46**(2), 39-49.
McDowell, G.R., Buchanan, J. and Lim, W.L. (2004), "Performance of ballast mixtures", *Ground Eng.*, **37**(10), 28-31.
McDowell, G.R. and Stickley, P. (2006), "Performance of geogrid-reinforced ballast", *Ground Eng.*, **39**(1), 26-30.
McMichael, P. and McNaughton, A. (2003), The stoneblower - delivering the promise; development, testing and operation of a new track maintenance system, *TRB 2003 Annual Meeting*, CD-ROM.
Mittal, S., Sharma, A.K., Lokesh, B.V. and Dwivedi, A. (2009), "Study of behaviour of ballast using geosynthetics", *Proceedings of the 4th Asian Regional Conference of Geosynthetics*, Shangai, China. Li, G., Chen, Y., and Tang, X., Editors, 656-661.
Pintner, R.M., Vinson, T.S. and Johnson E.G. (1987), "Nature of fines produced in aggregate processing", *J. Cold Reg. Eng.,* **1**(1), 10-21.
Raymond, G.P. and Bathurst, R.J. (1987), "Performance of large-scale model single tie-ballast systems", *Transport. Res. Record*, **1131**, 7-14.
Raymond, G.P. (2000), "Track and support rehabilitation for a mine company railroad", *Can. Geotech. J.*, **37**, 318- 332.
Szymoniak, T. (1986), *Reliability of the Dimethyl sulfoxide (DMSO) Accelerated Weathering Test to Predict the Degradation Characteristics of Basaltic Road Aggregates*, M.S. Dissertation, Department of Civil and Environmental Engineering, Oregon State University, Corvallis, Oregon.
Tannant, D.D. and Wang, C. (2004), "Thin tunnel liners modeled with particle flow code", *Eng. Computation.*, **21**(2/3/4), 318-342.
Vallejo, L.E. and Chik, Z. (2009), "Fractal and laboratory analyses of the crushing and abrasion of granular materials", *Geomech. Eng.*, **1**(4), 323-335.
Villard, P. and Chareyre, B. (2004), "Design methods for geosynthetic anchor trenches on the basis of true scale experiments and discrete element modelling", *Can. Geotech. J.*, **41**, 1193-1205.

*CC*